The role of 3D fault geometry in the rupture propagation and arrest during the 2016 Kaikoura (New Zealand) earthquake

Photos taken by Will Ries, Russ Van Dissen, Julian Thomson

Yoshihiro Kaneko, GNS Science (New Zealand)
Ryosuke Ando, University of Tokyo (Japan)

Rupture pattern during the Kaikoura EQ was very complex

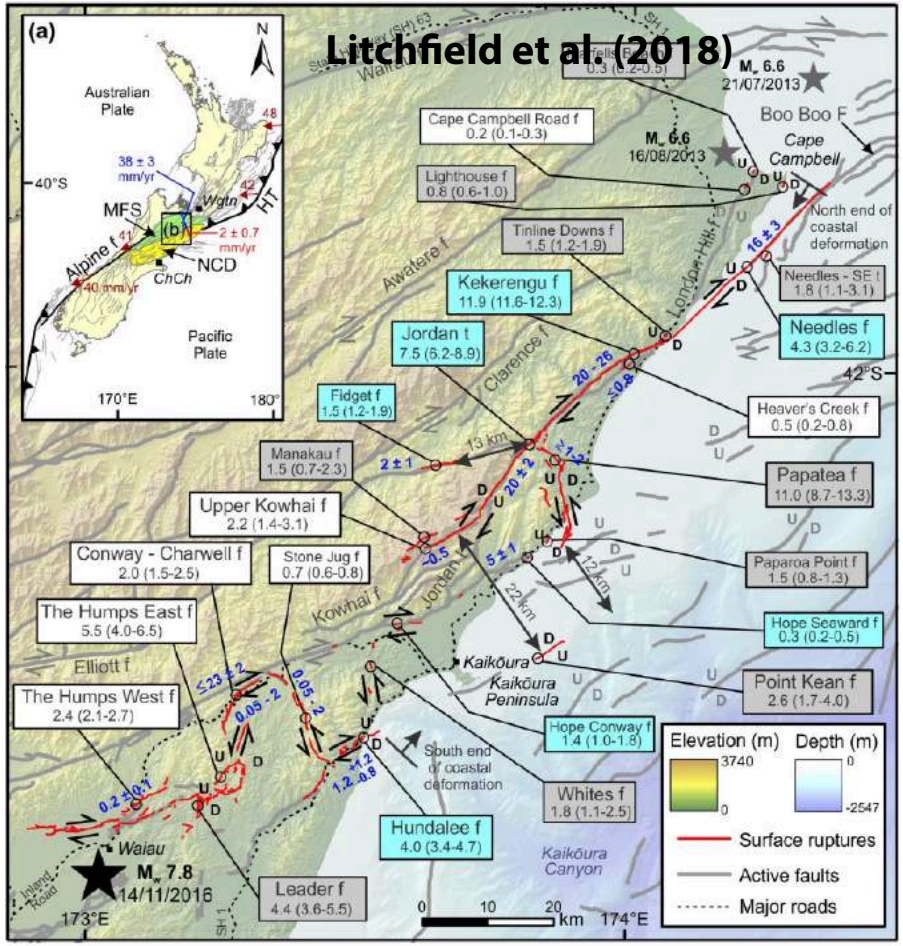

Slip model derived from the inversion of InSAR, GPS, LiDAR and coastal uplift

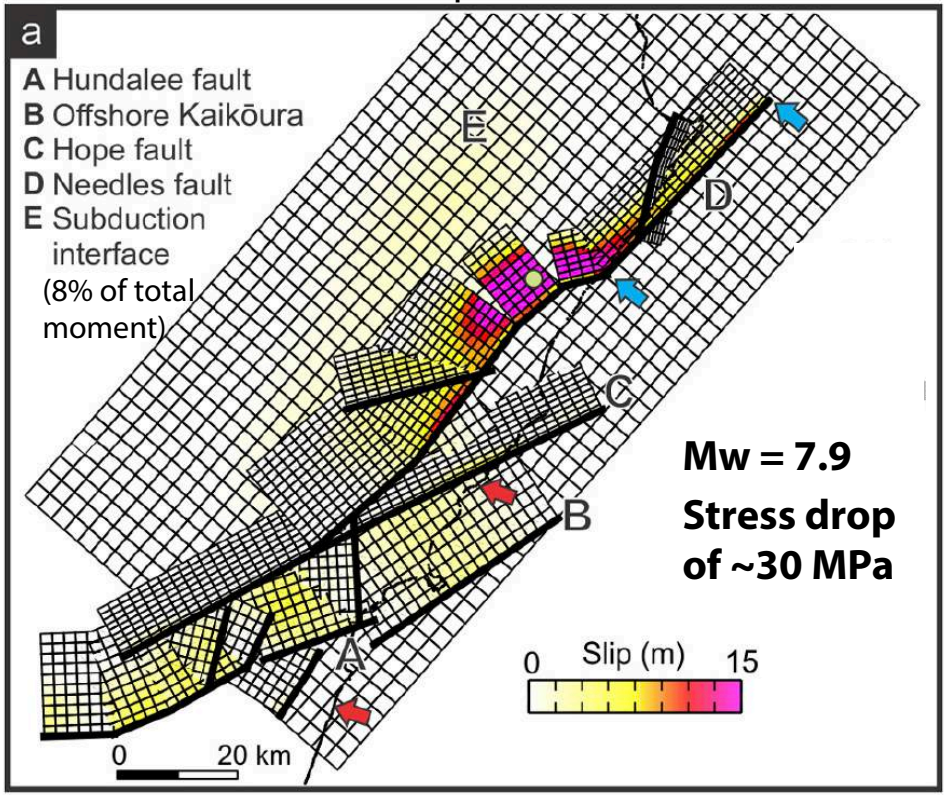

Clark et al. (2017), updated from Hamling et al. (2017)

Kinematic source models that fit well local waveforms

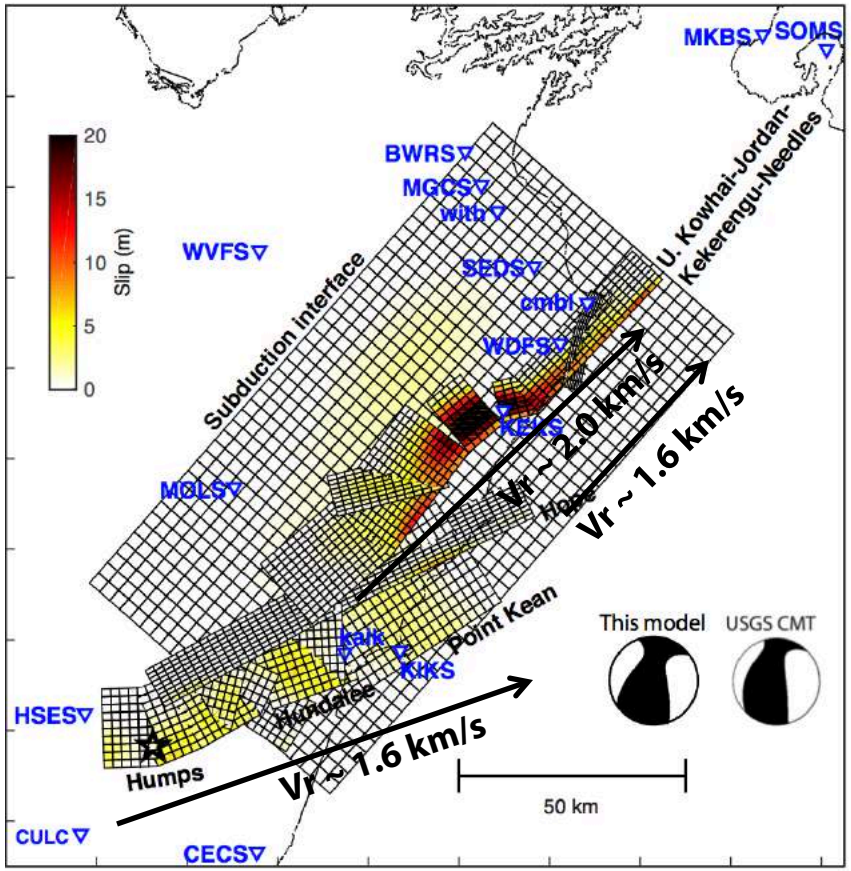

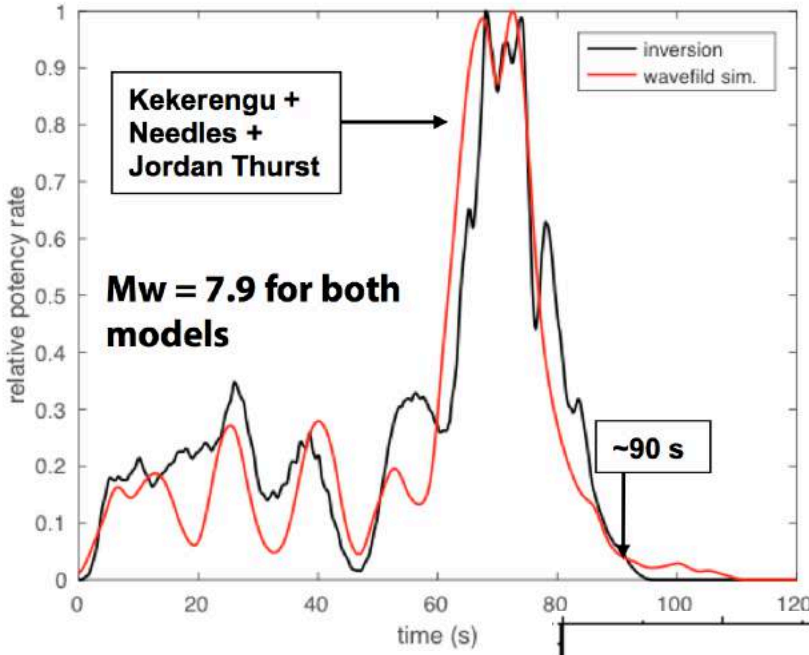

Holden, Kaneko, et al. (2017)

Slow rupture velocity (< 2.0 km/s) despite large stress drop

Largest moment release at 60–80 s

Consistent with other studies

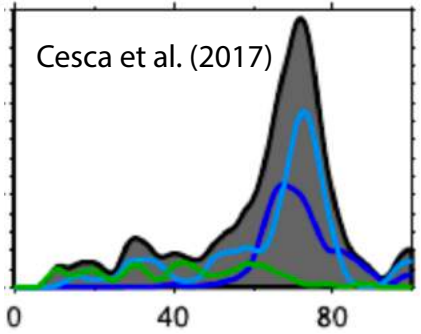

Model setup: Fault geometry for dynamic rupture simulations

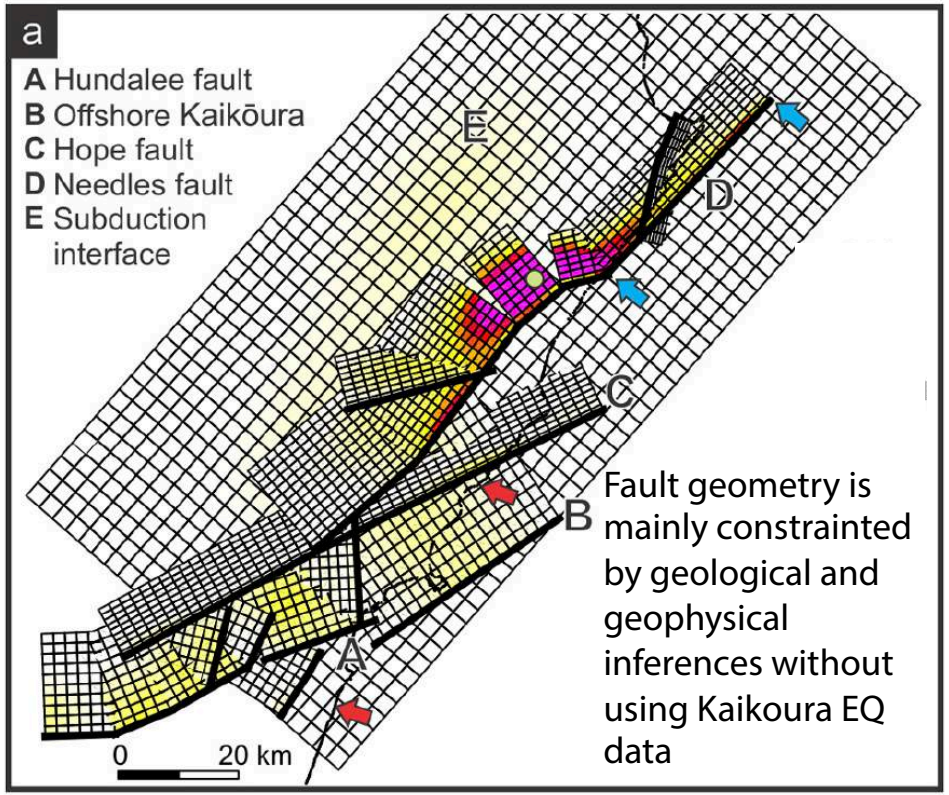

Fault geometry is mainly constrainted by geological and geophysical inferences without using Kaikoura EQ data

Clark et al. (2017), updated from Hamling et al. (2017)

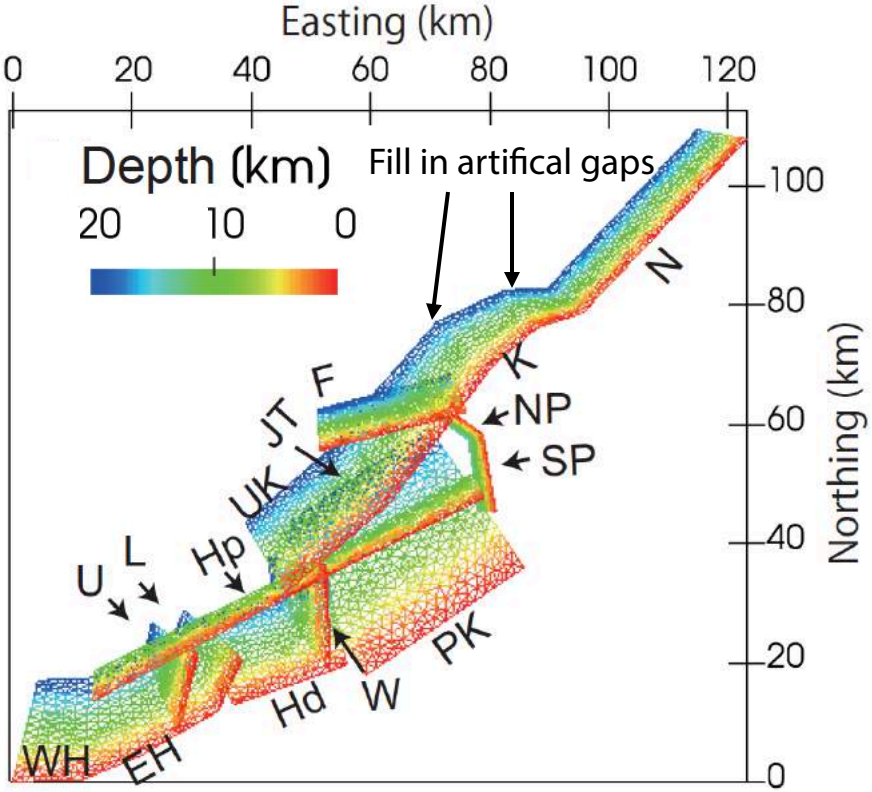

Assuemed fault geometry (A few minor faults removed; No subduction interface)

Model setup: Fault geometry for dynamic rupture simulations

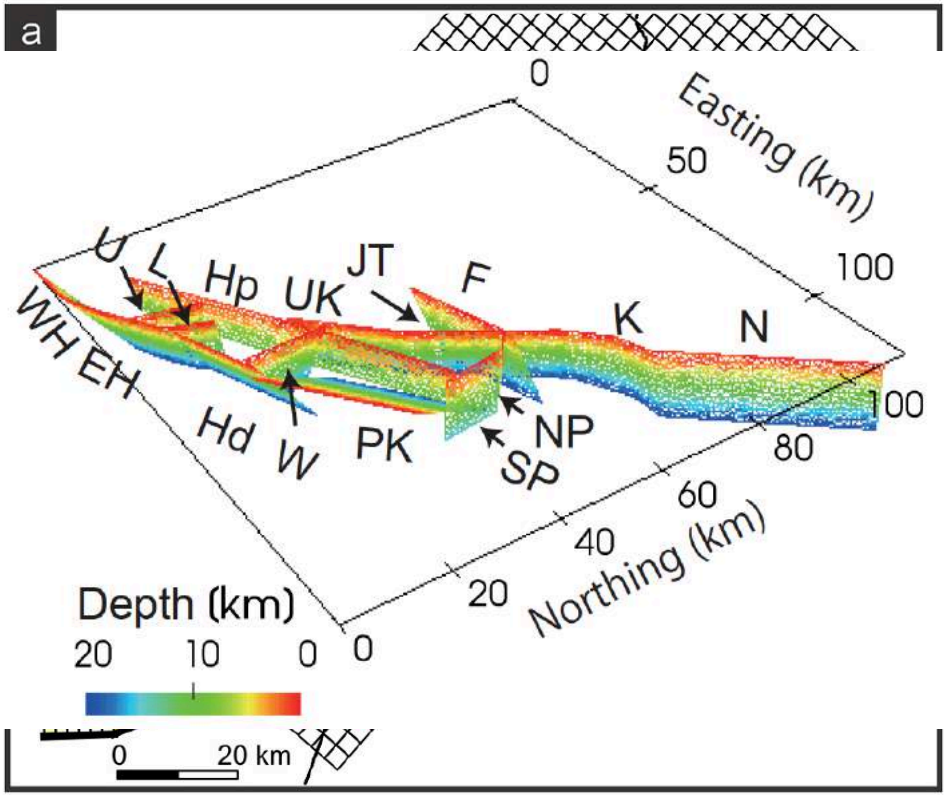

Clark et al. (2017), updated from Hamling et al. (2017)

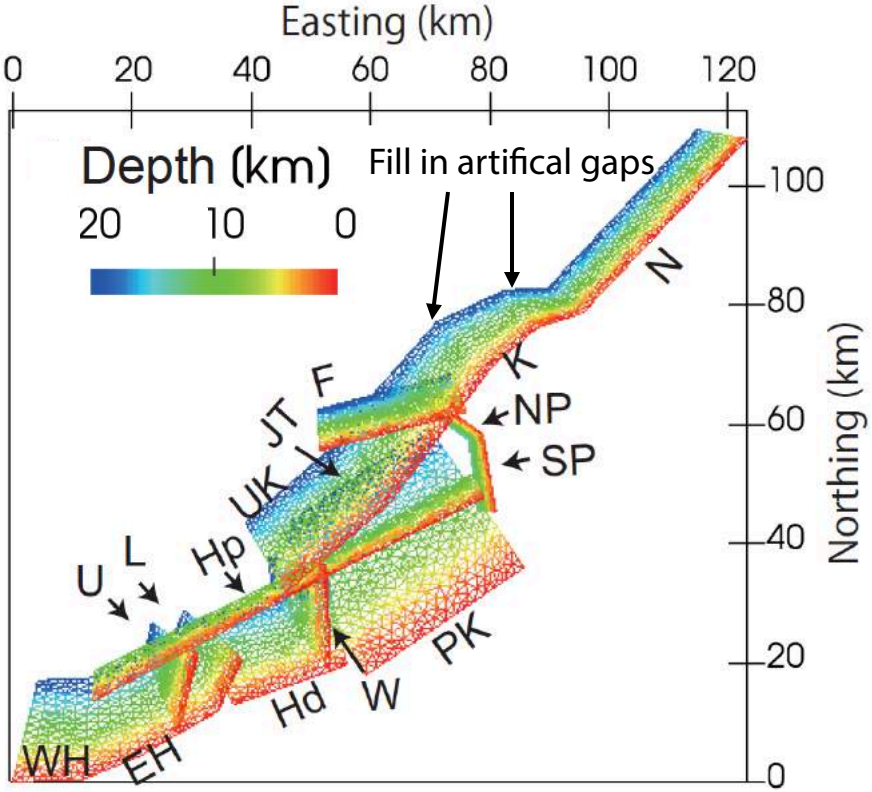

Assuemed fault geometry (A few minor faults removed; No subduction interface)

Important model constraint: Regional tectonic stress field

Focal mechanisms of EQs prior to the Kaikoura EQ

Orientation of principal stress axis

Stress ratio $v=(\sigma_1-\sigma_2)/(\sigma_1-\sigma_3)$

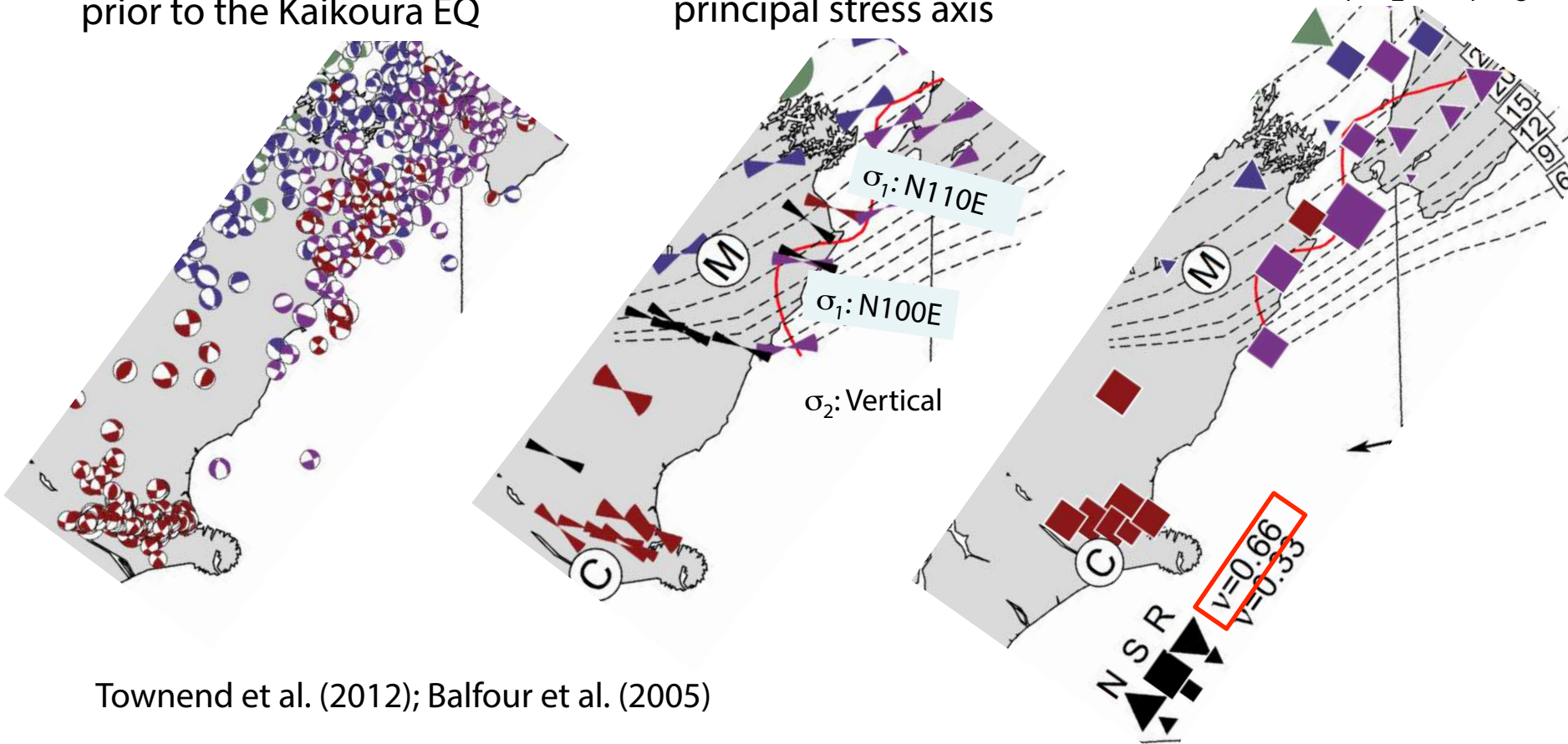

Townend et al. (2012); Balfour et al. (2005)

Initial stresses and fault friction parameters for representative cases

Absolute Stress vs. depth

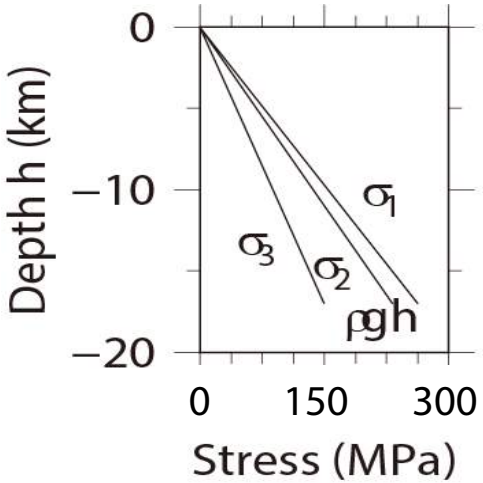

$\sigma_{vert}(z) = \sigma_2(z) = 17z$ [MPa/km]

Stress ratio $v = (\sigma_{Hmax}-\sigma_{vert})/(\sigma_{Hmax}-\sigma_{Hmin}) = 0.66$

$\sigma_{Hmin}/\sigma_{vert} = 0.74$ which results in the stress drop of ~10 MPa at hypocenter

Slip weakening friction law

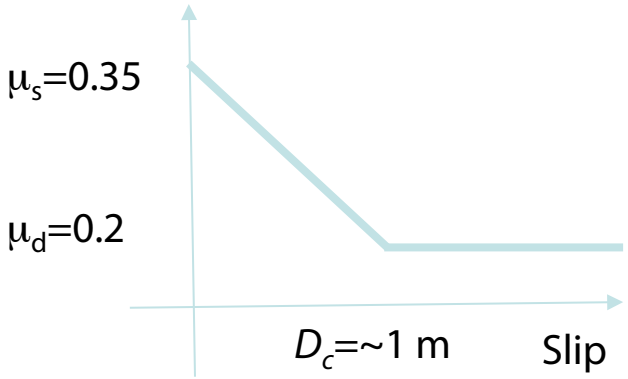

Uniform distributions of friction coefficients and Dc

Homogeneous elastic properties (Vp = 5.2 km/s, Vs = 3.0 km/s)

Neighboring parameter space also explored

Numerical method: Fast-Domain-Partitioning Boundary Integral Equation Method (Ando, 2016)

Analysis of potential stress-drop distribution (prior to simulation)

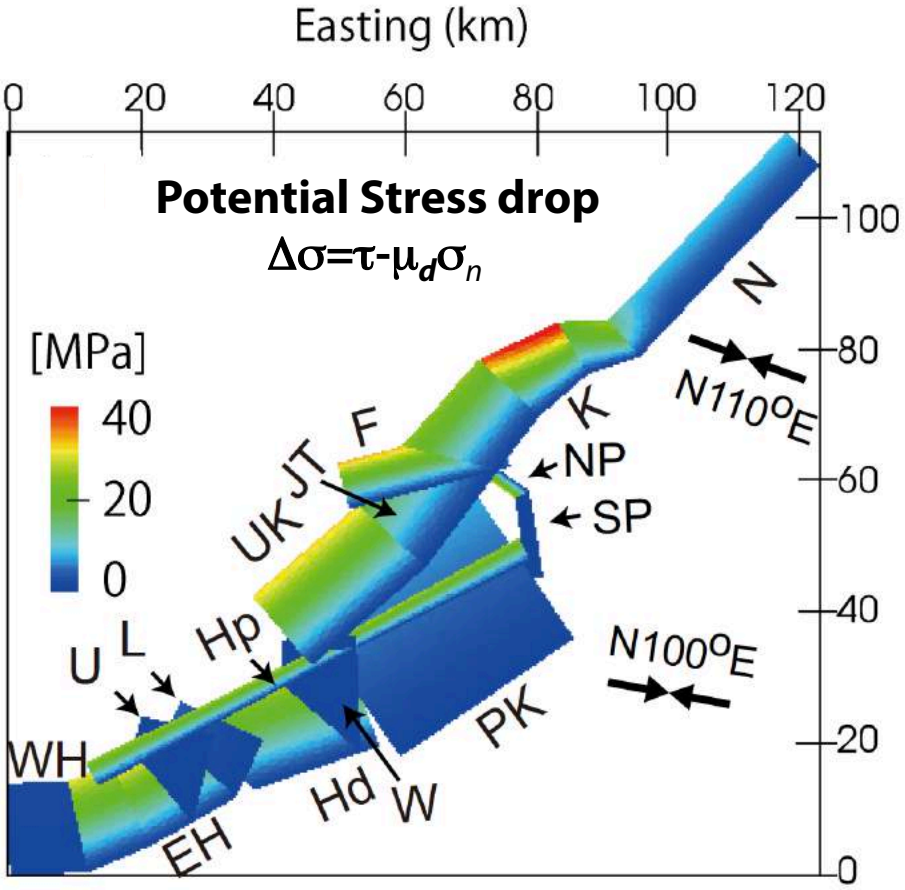

Spatially homogeneous:

- Regional stress (depth-dependent)
- Friction coefficients μ_s, μ_d
- Slip weakening distance Dc

Spatially heterogeneous:

- Shear and normal tractions
- Frictional strength
- Seismological fracture energy

Kekerengu (K) is the most optimally oriented fault

Hope (Hp) is also optimally oriented

Western Humps (WH) and Needles (N) are unfavorably oriented

Model reproduces spontaneous multi-fault rupture

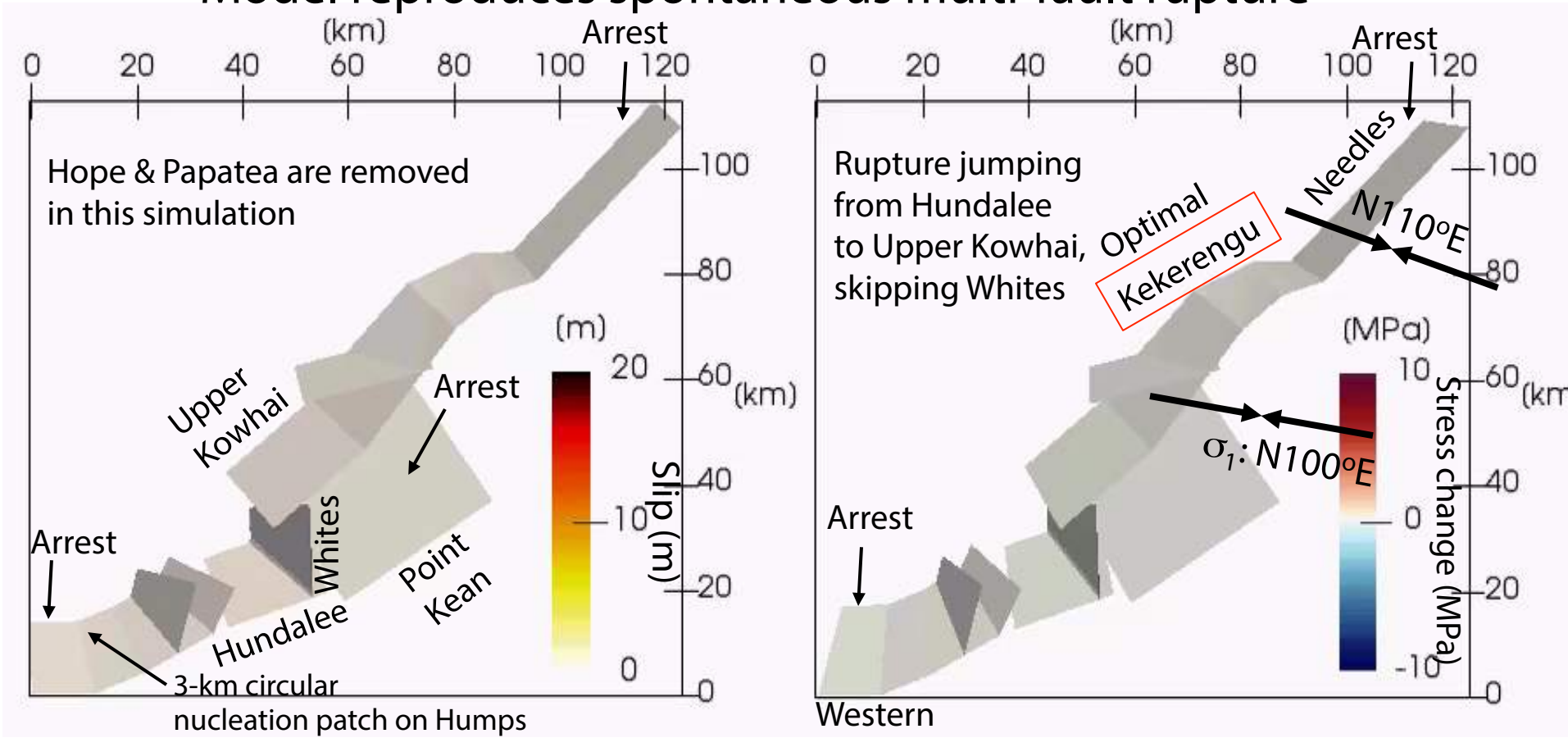

Comparison between simulated and inverted slip distributions

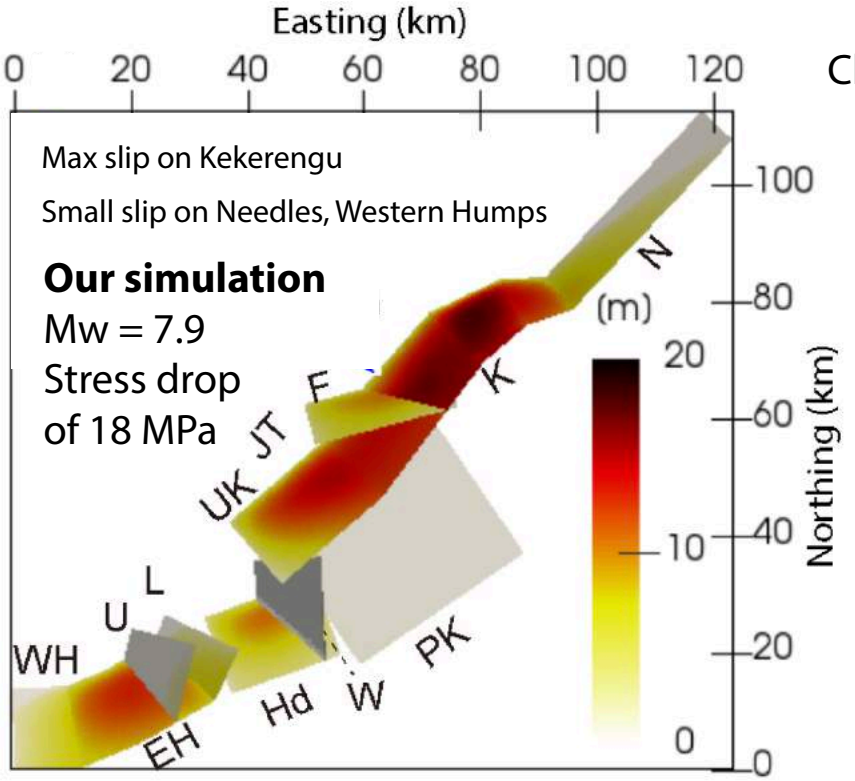

Clark et al. (2017), updated from Hamling et al. (2017)

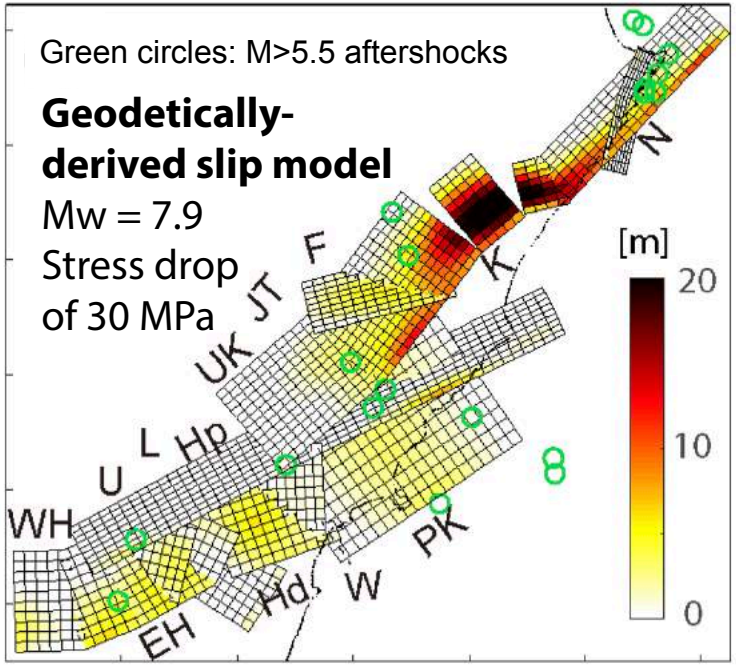

The model reproduces the primary features of the observationally estimated slip distribution.

Comparison between simulated and estimated rupture times

Assumption: Observed PGVs at near-fault stations (<10 km) are generated by propagating rupture front passing by the vicinity of these stations, and the same goes for the timings.

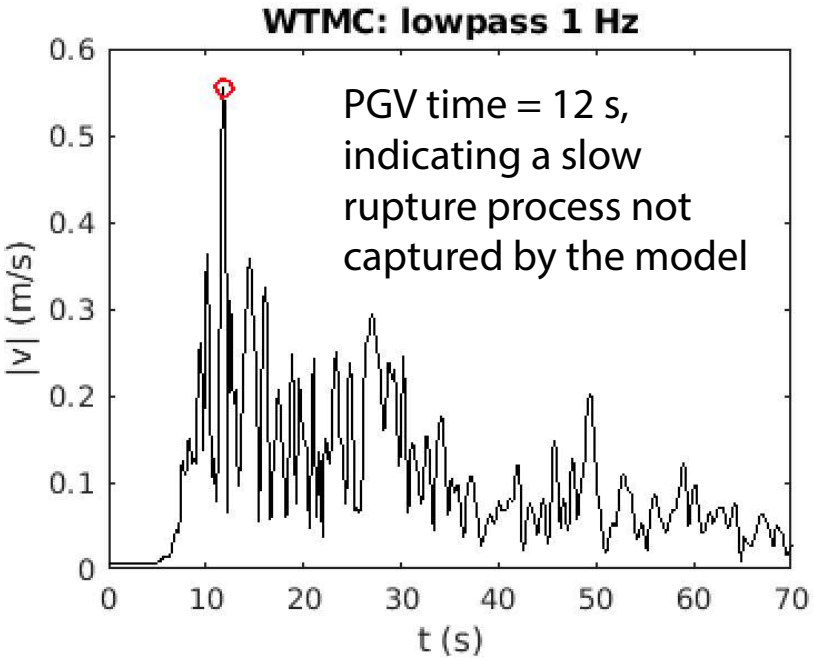

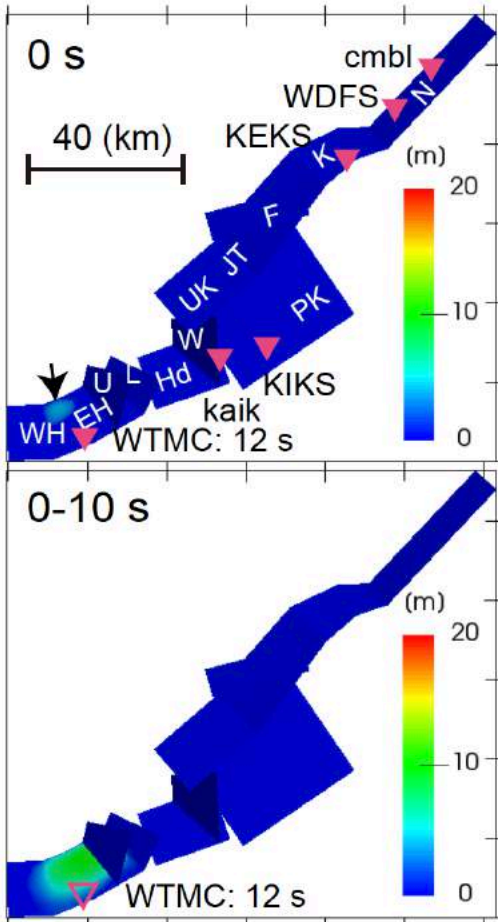

Colors: slip accumulated in the indicated 10 s intervals

Comparison between simulated and estimated rupture times

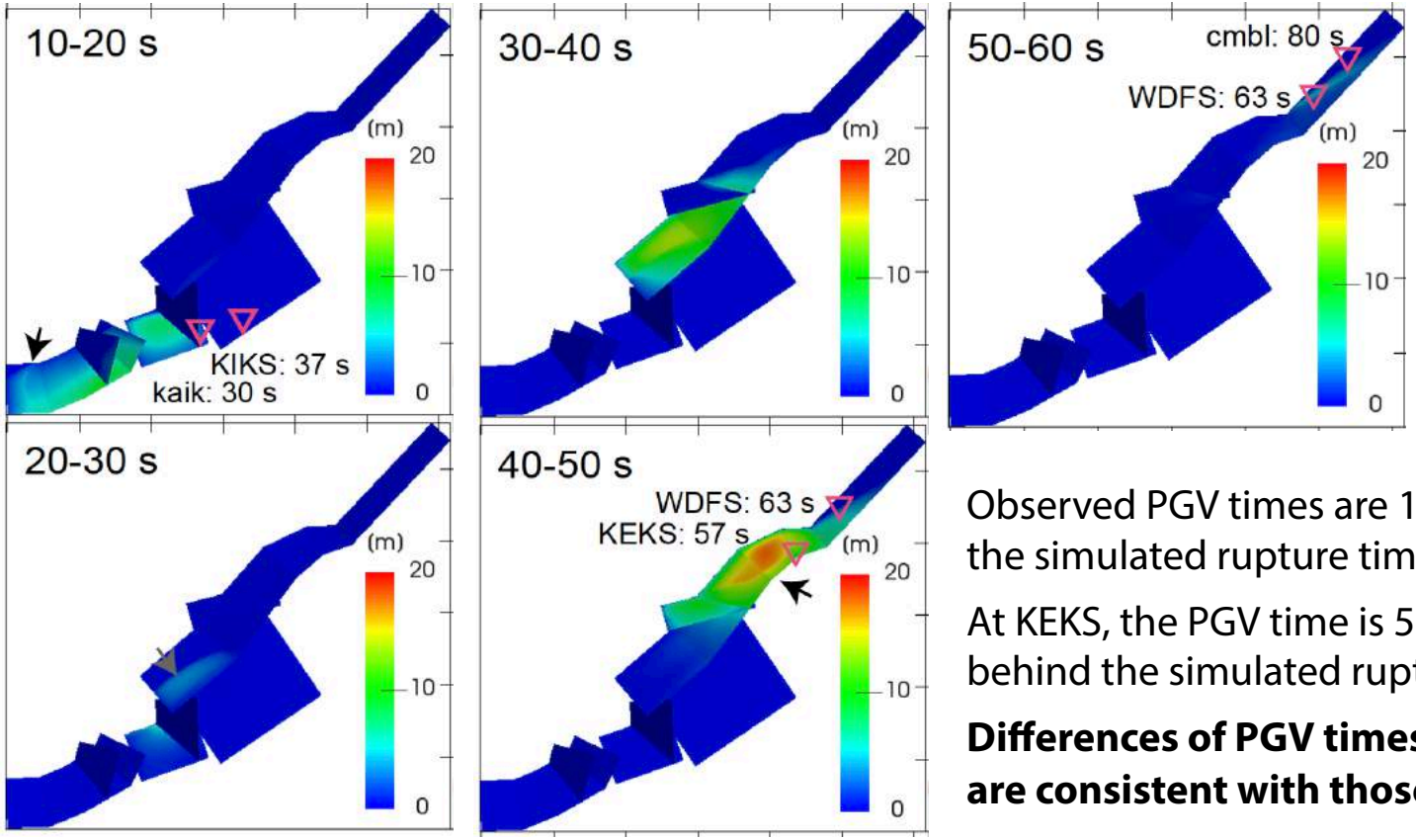

Colors: slip accumulated in the indicated 10 s intervals

Observed PGV times are 12-18 s slower than the simulated rupture times.

At KEKS, the PGV time is 57 s, which is ~15 s behind the simulated rupture time.

Differences of PGV times between stations are consistent with those in the simulation.

Comparison between simulated and inverted source time functions

Mw = 7.9 for all of them

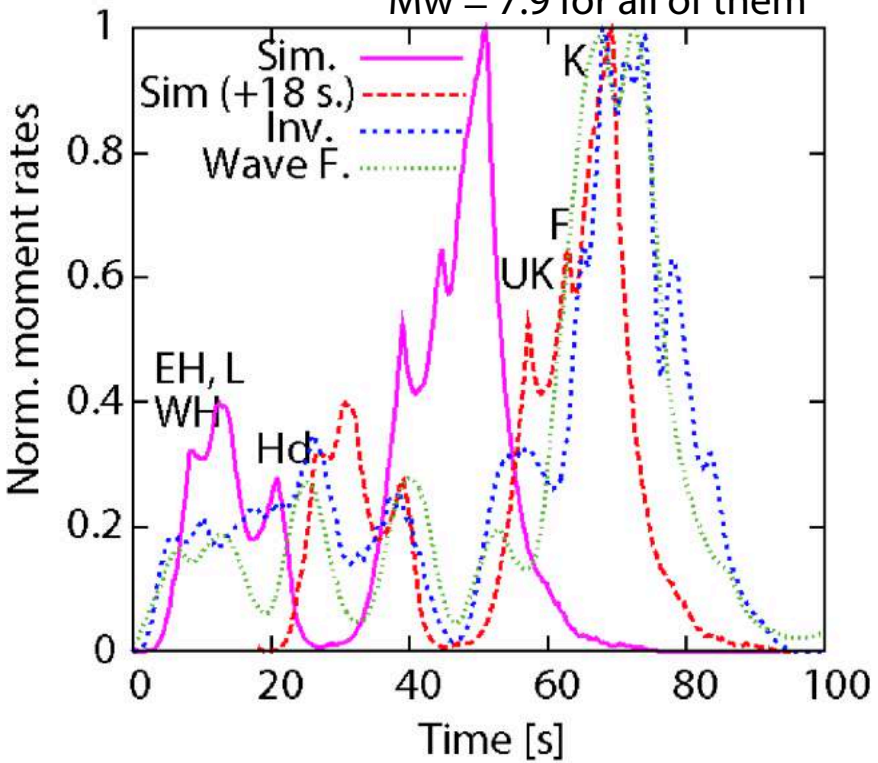

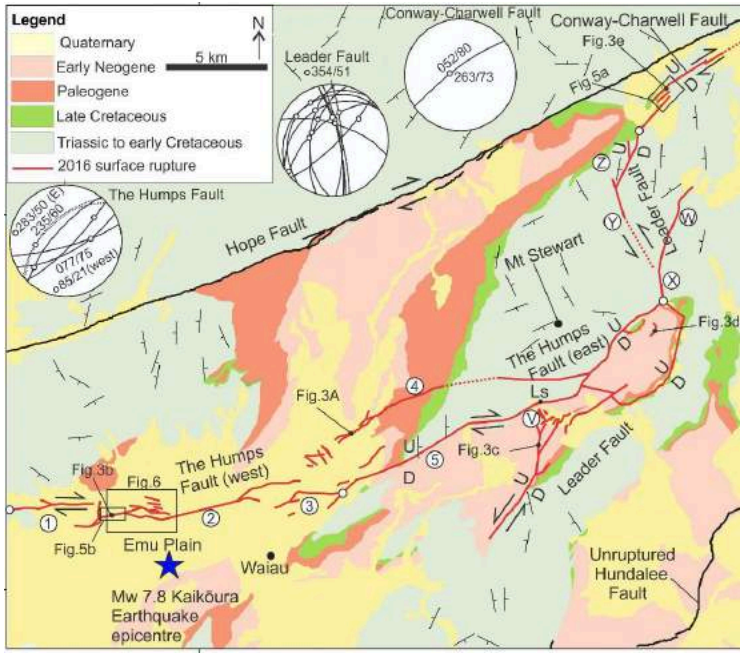

Refined location of the hypoceter (Nicol et al., 2018)

Simulated rupture duration is shorter than observationally inferred ones.

Shifting the simulated STF by 18 s (red curve) leads to a reasonable agreement in the overall shape.

Longer source duration may be caused by more complex rupture nucleation south of Humps.

Simulation with the Papatea fault

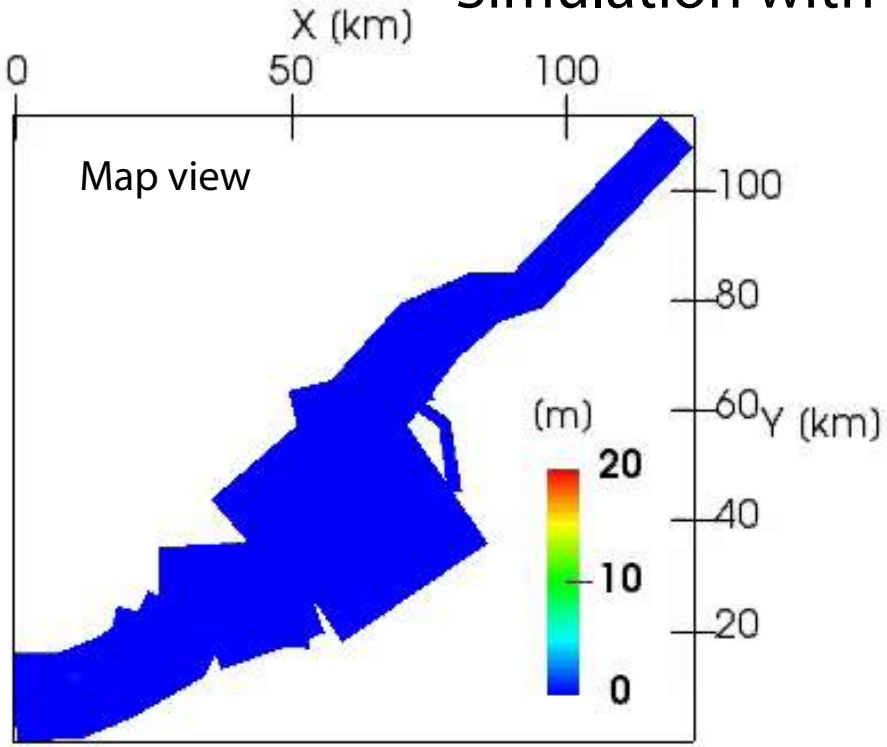

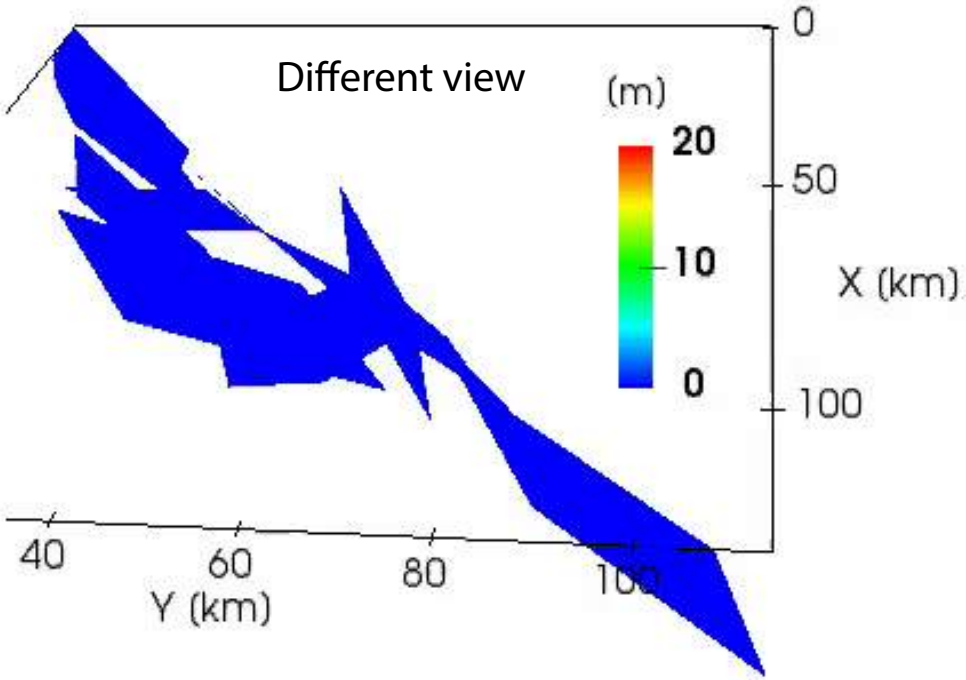

Although the northern part of Papatea is favorably oriented and generates slip, its southern part connecting Point Kean is at unfavorable orientation.

Our model implies that the Papatea fault did not play a dominant role in the rupture transfer from the southern to the northern fault segments.

Simulation with the Hope fault

The optimally-oriented Hope fault produces large slip (>10 m), which was not observed.

Hope Fault may not have been fully reloaded at the time of the Kaikoura EQ, since it was ruptured by the 1888 Amuri EQ (or 1780 M>7 EQ) and the recurrence interval of 180-310 years (Langridge et al, 2003).

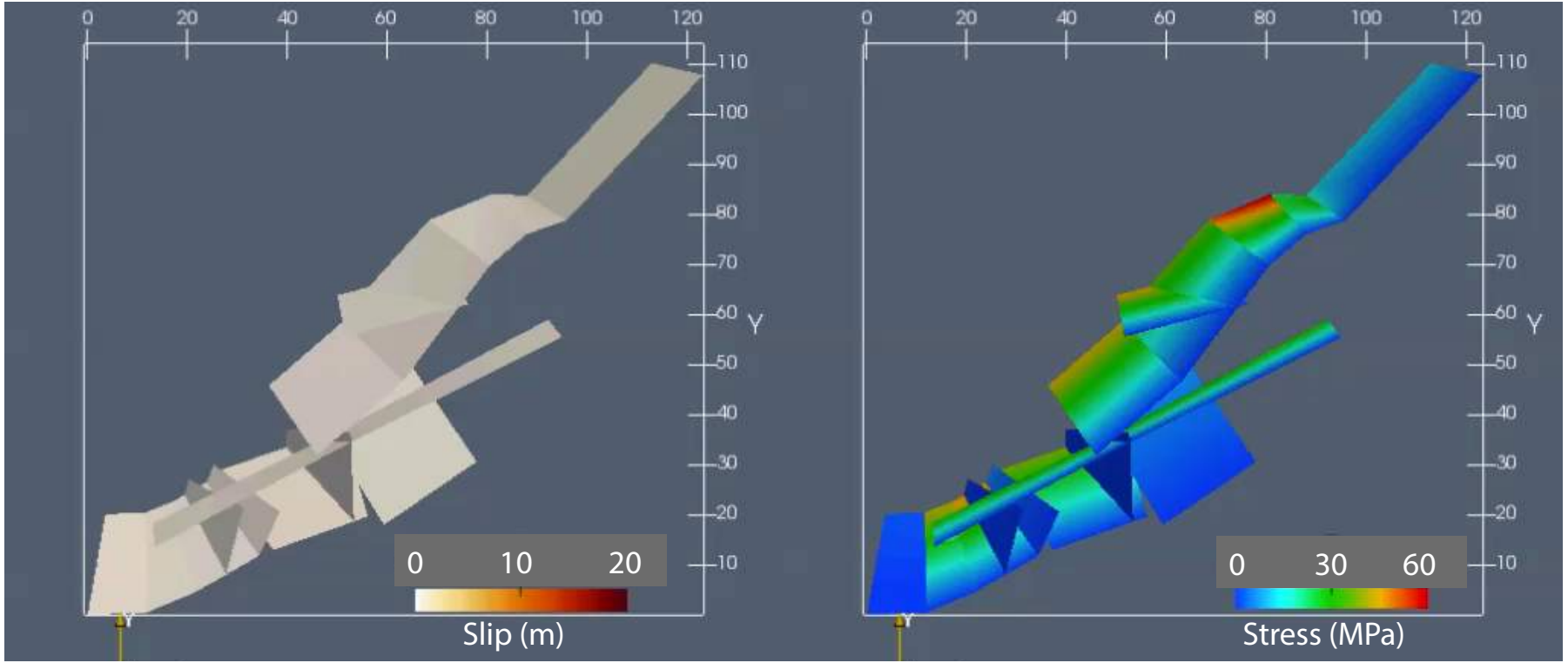

Implication #1: Rupture arrest due to unfavorable fault orientations

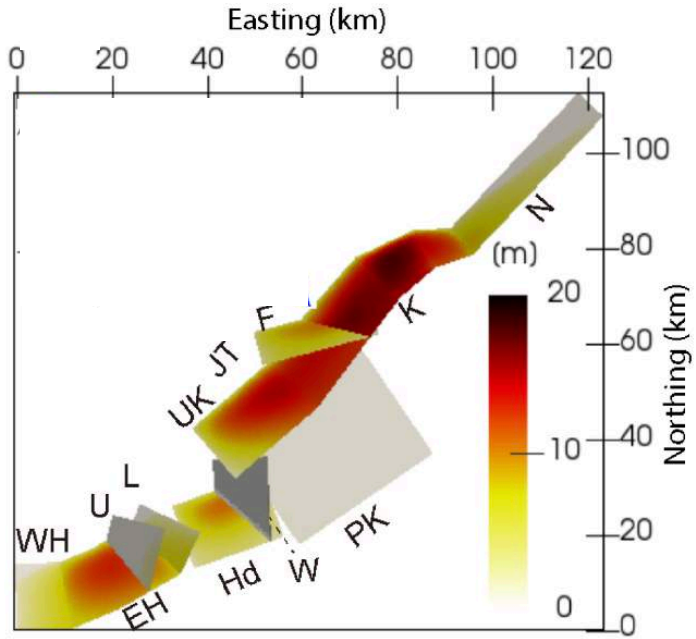

Rupture arrest is more likely to occur on unfavorably oriented faults.

Bouchon et al. (1998) used kinematic analysis and argued that Landers EQ rupture was arrested by the unfavorable orientations of Emerson/Camp Rock Faults.

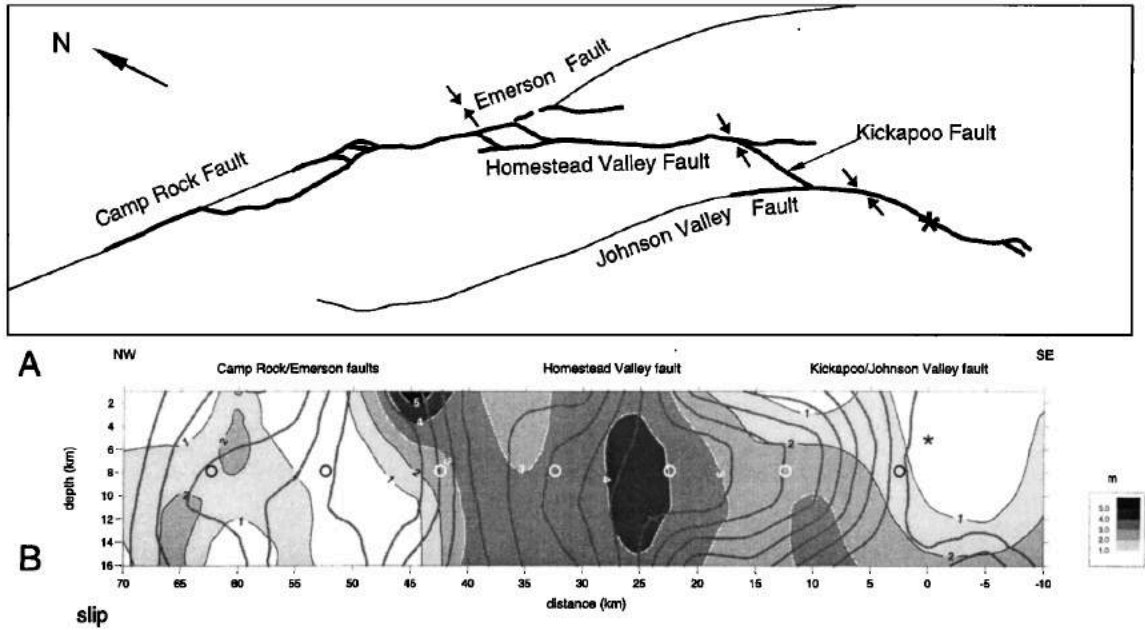

Implication #2: Identifying seismic asperities prior to major EQs

There are many other faults in this region that could be ruptured during major earthquakes.

Since the final slip distribution is well predicted by potential stress drops (except Hope), one might be able to use potential stress drops and paleoseismic records to identify seismic asperities prior to major EQs (More testing is needed).

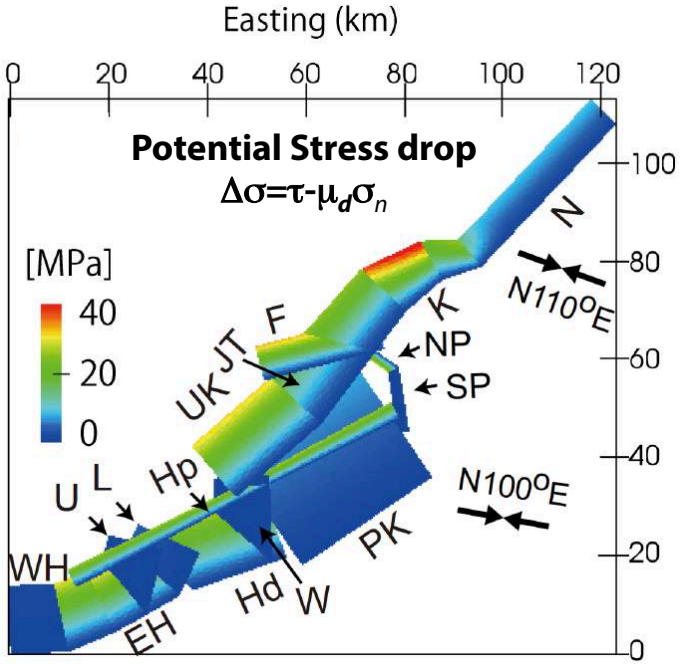

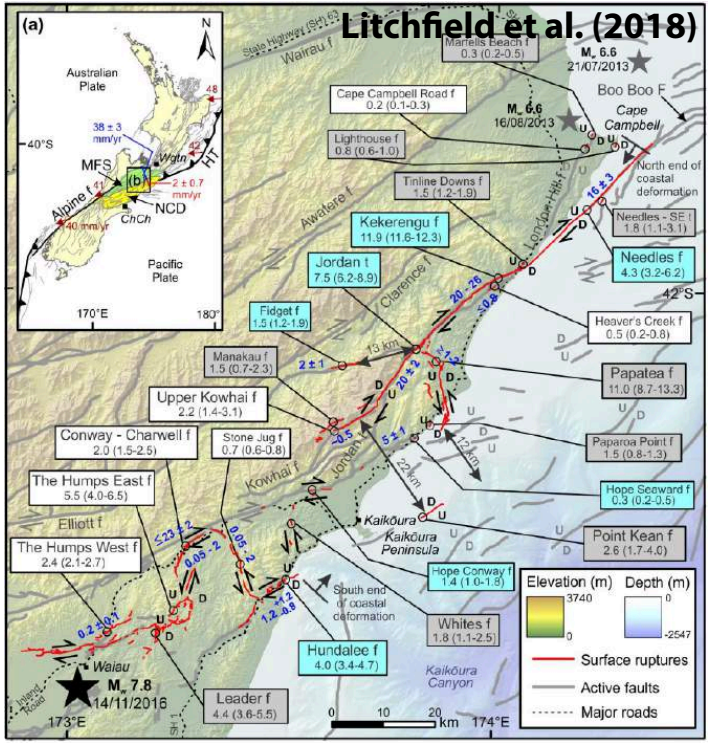

Conclusions

- Relatively simple dynamic model considering realistic fault geometry and regional stress field reproduces multi-fault rupture during the Kaikoura EQ.
- Our model shows spontaneous rupture arrest on the western Humps and Needles faults, which are unfavorably oriented in a regional stress field.
- The rupture may have jumped over 13 km from the Hundalee to Upper Kowhai fault. Such large rupture jump might have been due to the large seismogenic width (e.g., Bai and Ampuero, 2017).
- The Hope fault, the most active fault in the region, may not have been fully reloaded at the time of the Kaikoura EQ and hence was not ruptured.
- Our results illuminate the importance of 3D fault geometry in understanding the dynamics of complex, multi-fault rupture events.

Ando & Kaneko (a manuscript resubmitted after minor revision)

Extra slides

Potential stress-drop distribution on the subduction interface

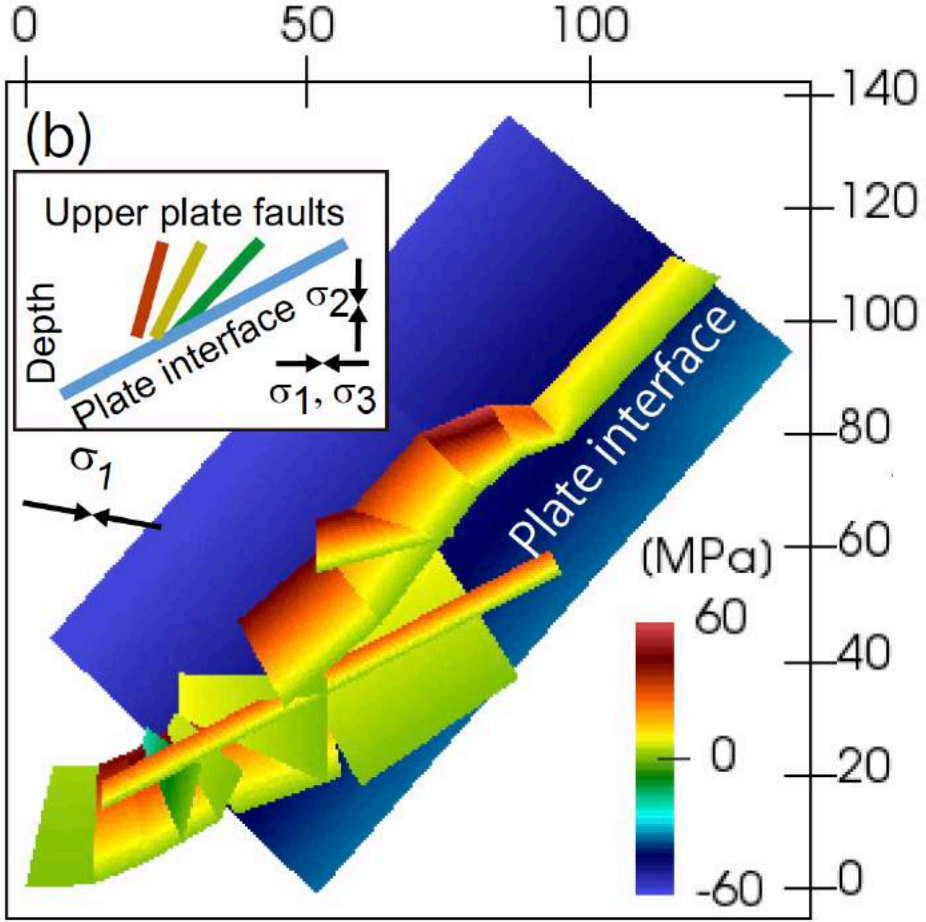

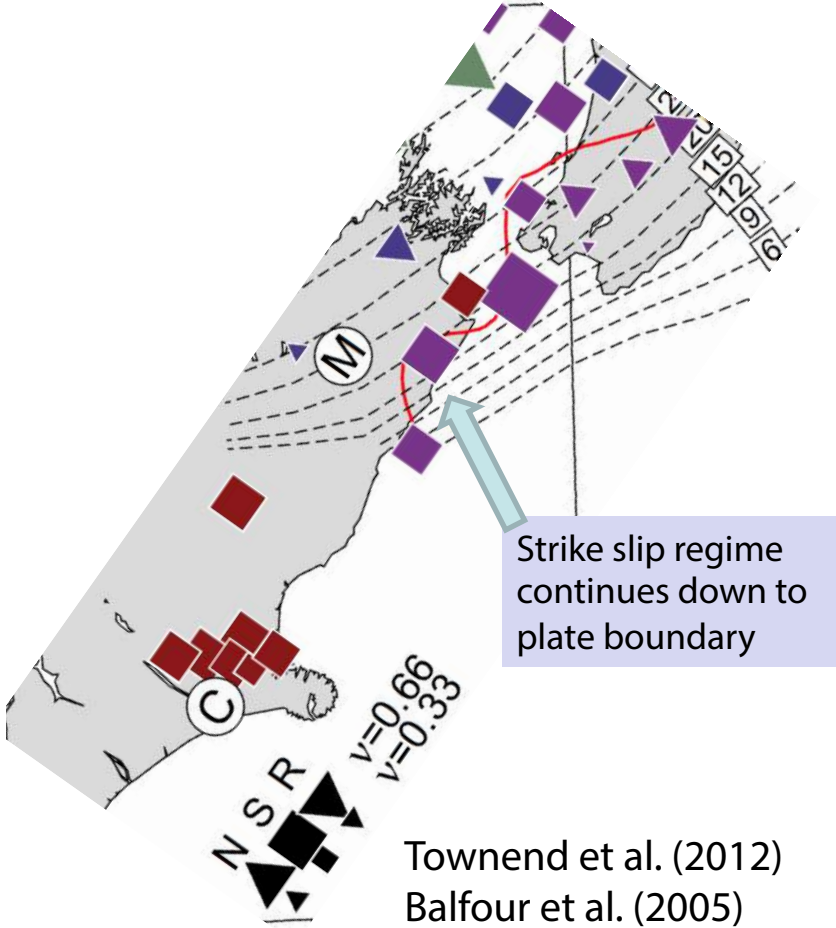

Townend et al. (2012)
Balfour et al. (2005)

Difference of 10° in principle stress axes slightly changes the potential stress drops

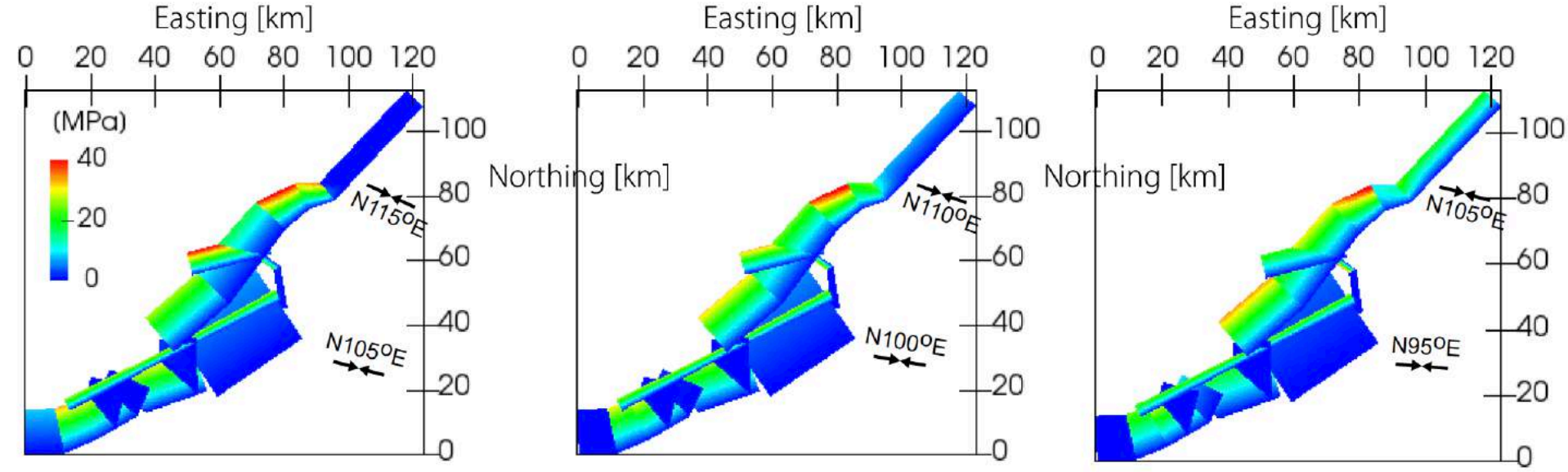

Comparison between simulated and inverted rake angle distributions

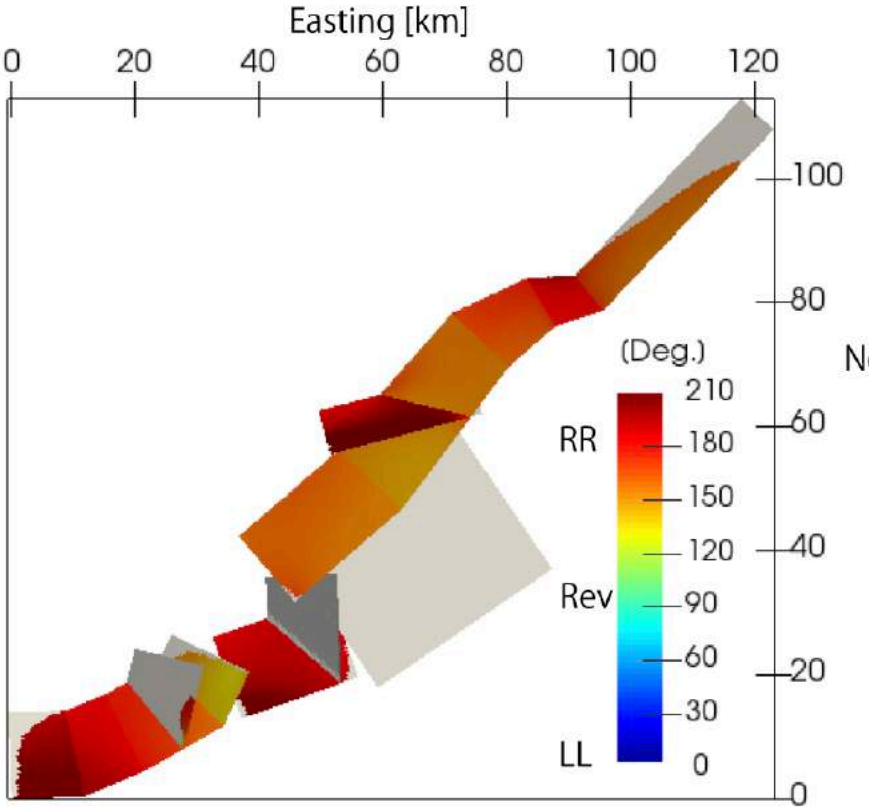

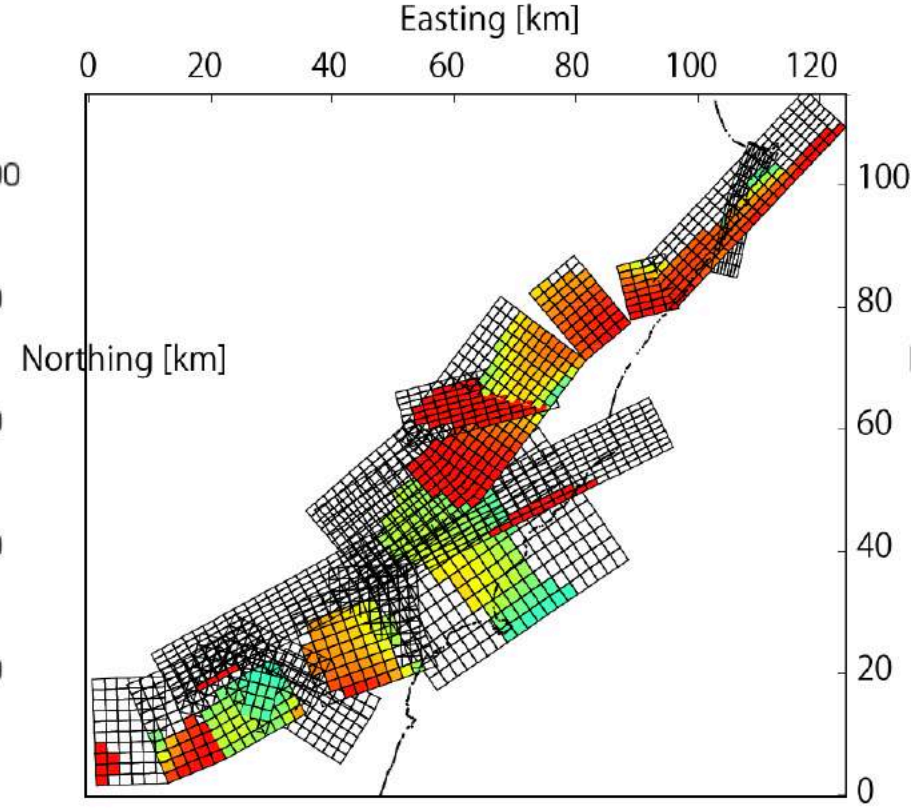

Parameters explored in this study

Model name	μ_s	D_c (m)	Stress ratios σ_{hmin}/σ_v	M_w	Dynamic triggering*
S	0.35	1.0	0.74	7.9	Yes
A	0.35	1.7	0.73	8.0	Yes
B	0.32	0.5	0.76	7.8	Yes
S’	0.35	1.2	0.74	7.5	No
A’	0.35	1.8	0.73	7.6	No
B’	0.35	0.5	0.76	7.4	No